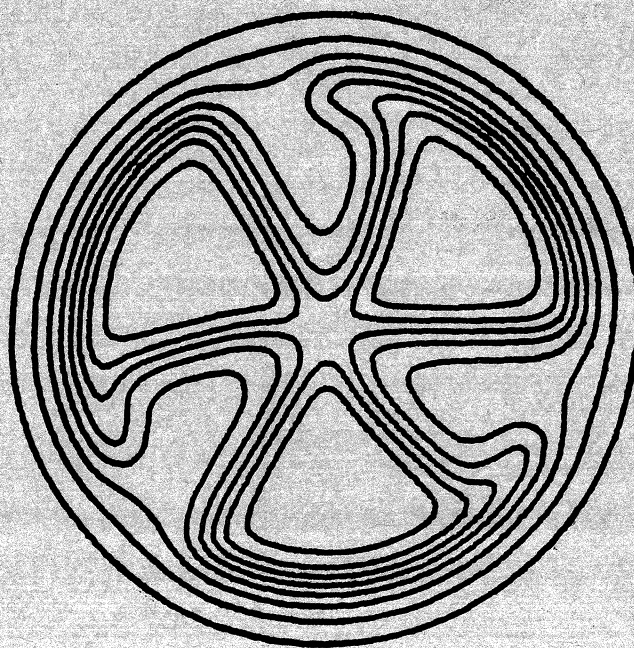


MICHIGAN STATE UNIVERSITY

CYCLOTRON LABORATORY

STUDY OF THE  $^{37}\text{Cl}(p, ^3\text{He})^{35}\text{S}$  REACTION

A. GUICHARD, H. NANN and B.H. WILDENTHAL





## Study of the $^{37}\text{Cl}(p, ^3\text{He})^{35}\text{S}$ Reaction\*

A. Guichard,\*\* H. Mann and B. H. Wildenthal  
Cyclotron Laboratory  
Michigan State University, East Lansing, Michigan 48824

### I. INTRODUCTION

Information<sup>1-7</sup> on  $^{35}\text{S}$  is rather scarce. Excitation energies of levels up to 7.022 MeV have been determined by Moss<sup>1</sup> via the  $^{34}\text{S}(d,p)$  reaction. Values of the single-neutron angular momentum transfer  $\lambda_n$  to a few levels have been deduced from study of the same reaction by van der Baan and Leighton.<sup>2</sup> Measurements of particle- $\gamma$  angular correlations from the  $^{34}\text{S}(d,p\gamma)$  reaction<sup>3</sup> have yielded a few spin assignments or spin limits.

Shell-model calculations have been performed by several authors on this nucleus. The negative-parity states have been studied first by Erne<sup>8</sup> and more recently by Maripuu and Hokken.<sup>9</sup> The latter authors assume a  $^{32}\text{S}$  core and  $d_{3/2}^2 f_{7/2}$  and  $d_{3/2}^2 p_{3/2}$  configurations, while only the  $d_{3/2}^2 f_{7/2}$  configuration was assumed by Erne. Positive-parity states have been calculated by Glaudemans *et al.*<sup>10</sup> and Wildenthal, *et al.*<sup>11</sup> A full s-d vector space is assumed in the calculations of Wildenthal, *et al.* together with several different effective Hamiltonians.

NUCLEAR REACTIONS:  $^{37}\text{Cl}(p, ^3\text{He})^{35}\text{S}$ ,  $E_p=40.2$  MeV; measured ( $E_{^3\text{He}}, \theta$ ); enriched target.  $^{35}\text{S}$  deduced levels, L values.

The present  $^{37}\text{Cl}(p, ^3\text{He})$  experiment was undertaken with the aim of augmenting the existing experimental information on  $^{35}\text{S}$ .

Determination of the two-nucleon angular momentum L transferred to a level will determine the parity and limit the possible values of the spin assignments for levels about which nothing was previously known beyond the excitation energy. Moreover, to the extent that the reaction mechanism is understood, the validity of the shell-model wave functions for the low-lying levels can be investigated via comparison of the shapes and magnitudes of theoretical angular distributions to the observed

Angular distributions of the  $^{37}\text{Cl}(p, ^3\text{He})^{35}\text{S}$  reaction at

40.2 MeV bombarding energy have been measured for states in  $^{35}\text{S}$  up to 9.16 MeV energy excitation. These data have been analysed with the distorted-waves Born approximation and values of the angular momentum L transferred to several states have been deduced. A shell-model analysis of the transitions to the low-lying levels has been performed and the new information gained about the structure of  $^{35}\text{S}$  is discussed.

\* Supported in part by the United States National Science Foundation.

\*\* On leave of absence from Institut de Physique Nucleaire de Lyon-France.

data. The only previously existing  $^{37}\text{Cl}(p, ^3\text{He})^{35}\text{S}$  data consisted of the angular distribution of the transition to the ground state, reported by Vignon, et al.<sup>12</sup>

## II. EXPERIMENTAL PROCEDURE

The experiment was performed with 40.2 MeV protons from the Michigan State University Cyclotron. The target, of Na Cl, was isotopically enriched in  $^{37}\text{Cl}$  (97%), and the thickness of  $^{37}\text{Cl}$  was  $\sim 55 \text{ g/cm}^2$ . It was fabricated by evaporation of the salt onto a carbon backing ( $30 \text{ }\mu\text{g/cm}^2$ ). The reaction products were detected with a wire-counter, plastic-scintillator combination placed in the focal plane of an Enge split-pole spectrograph.

With this arrangement, good particle identification and an energy resolution of about 30 keV was obtained. A typical spectrum, obtained at  $15^\circ$ , is presented in Fig. 1; levels up to 9.16 MeV have been observed.

Angular distributions measured for various residual levels, taken between  $4^\circ$  and  $50^\circ$ , are displayed in Figs. 2 and 3. Error bars reflect only statistical uncertainties. The  $(p, ^3\text{He})$  cross-sections were determined by reference to the elastic scattering of protons, measured between  $27^\circ$  and  $49^\circ$ . The observed elastic scattering cross-sections were assumed to be equal in magnitude to those computed from the parameters of Greenlees, et al.<sup>13</sup> The observed and calculated shapes of the elastic scattering do match each other. The relative rates of the  $(p, p)$  and  $(p, ^3\text{He})$  reactions, measured under essentially identical experimental conditions, were then used to establish the cross section scale

for the  $(p, ^3\text{He})$  data. We estimate such a procedure to be accurate to 20%.

## III. DISTORTED WAVE ANALYSIS

The theoretical cross-sections for the  $^{37}\text{Cl}(p, ^3\text{He})^{35}\text{S}$  reaction have been calculated with the code DWUCK.<sup>14</sup> The two-nucleon form factor is computed according to the Bayman-Kallio method.<sup>15</sup> The optical parameters used in the present analysis are listed in Table I. The proton parameters are a modification of those of Greenlees and Pyle<sup>13</sup> and the  $^3\text{He}$  parameters are adapted from those of Morsch and Santo<sup>16</sup>. The cross-section for a  $A(p, ^3\text{He})B$  reaction is given by the following formula:

$$\frac{d\sigma}{d\Omega} = D_0^2 \times 9.72 \int_{LSJT} \frac{1}{2} \langle T_B | T_A \rangle^2 |D(S, T)|^2 \frac{(2S+1)}{2(2J+1)} \sigma_{LSJT}^{DW}(\theta) \quad (1)$$

where  $\sigma_{LSJT}^{DW}$  is the cross-section calculated by the code DWUCK for a given set of quantum numbers LSJT of the n-p pair. The coefficient  $D_0^2$  is a normalization factor related to the zero-range assumption of the interaction of the incident proton with the center of mass of the n-p pair. The value of  $D_0^2$  is not yet well known but has been empirically determined to be in the range 20-30. For levels where shell model wave functions are available, the theoretical cross-section (1) will be computed without  $D_0^2$  and, instead,  $D_0^2$  will be determined by comparison with the experimental cross section. The constant 9.72 comes from the normalization procedure of Baer, et al.<sup>17</sup> and is related to the range parameter of the two body interaction and to the size of the outgoing particle. The quantity  $D(S, T)$  is related

to the spin-isospin strength of the interaction potential; the values of Gillet<sup>18</sup> (with  $|D(0,1)|^2=0.72$  and  $|D(1,0)|^2=0.30$ ) have been used.

#### IV. RESULTS AND DISCUSSION

Our experimental results with L assignments are given in Table II. We have also included the information on excitation energies and  $J^\pi$  assignments as summarized by Endt and van der Leun<sup>19</sup> and the results of the (d,p) experiment from van der Baan and Leighton.<sup>2</sup> For the previously known levels, our excitation energies agree quite well with those reported by Endt and van der Leun. Our excitation energy scale was established by reference to the ground state and two levels the excitation energy of which are accurately known: 1572 and 3421 keV. The values of the presently assigned excitation energies are accurate to within 10 keV. Previously unobserved levels found in this experiment are noted in Table II (levels 14, 17, 21, 22, and 23.) The origin of such levels from the presence of the  $3\% \text{ }^{35}\text{Cl}$  in the target must be ruled out, of course. This is done by noting that some levels of  $^{33}\text{S}$  are indeed observed in this experiment, as can be seen in Fig. 1. Since these states in  $^{33}\text{S}$ , at 840, 2870 and 2970 keV are known<sup>20</sup> to be the most strongly populated in  $^{35}\text{Cl}(p, \text{}^3\text{He})^{33}\text{S}$ , one can then reasonably presume that levels with maximum cross-section greater than these known  $^{33}\text{S}$  levels belong to  $^{35}\text{S}$ . For the new levels observed above 7.022 MeV, the same sort of criterion was applied, this time with respect to  $^{23}\text{Na}(p, \text{}^3\text{He})^{21}\text{Ne}$ . Levels of  $^{21}\text{Ne}$  arising from

the presence of  $^{23}\text{Na}$  were also recognized by their kinematic shift. However, at higher excitation energies in the  $^{21}\text{Ne}$  spectrum, the level density and average cross sections are such as to obscure parts of the  $^{35}\text{S}$  spectrum beyond redemption. We note that new levels of  $^{21}\text{Ne}$  not reported in Ref. 19 are present in our spectra (for example the strong transitions to 8270 and 8330 keV.) Other weak unreported  $^{21}\text{Ne}$  transitions may also be present and, together with the strong levels, make the unambiguous identification of  $^{35}\text{S}$  levels quite difficult at these higher excitation energies.

A. Levels at  $E_x=0, 1575, 2717, 2938, 3421, 3598, 8430$  and  $9155$  keV.

In Fig. 4 we have represented the experimental level scheme observed in this experiment with the positive-parity level scheme arising from shell model calculations by Wildenthal et al.<sup>11</sup> and Wildenthal and Chung.<sup>21</sup> Calculation I (notation " $12.5 p+0^{17}$ " in ref. 11) assumes a  $^{16}\text{O}$  core plus a full sd basis; calculation II (ref. 21) has been performed in a hole formalism assuming a  $^{40}\text{Ca}$  core. These two methods give the same spin sequence below 4 MeV. For the positive-parity states only the spin of the ground state ( $3/2^+$ ) and of the 1575 keV ( $1/2^+$ ) have been yet determined; spin limits have been given for a few other states. We have identified six levels observed in the (p,  $^3\text{He}$ ) experiment with levels in the calculated spectra. Assuming the correspondence, we can compare the experimental

cross-sections to the one predicted from DWBA calculations based on the mentioned shell-model wave functions. The spectroscopic amplitudes calculated with the two sets of shell model wave functions are listed in Table III (calculation I) and Table IV (calculation II).

In the simplest applicable shell model ( $^{32}\text{S}$  core),  $^{37}\text{Cl}$  is represented by  $\pi d_{3/2} \nu d_{3/2}^4$  and the  $^{35}\text{S}$  ground state by  $\nu d_{3/2}^3$ . The two-nucleon pick up connection thus should involve essentially a  $(d_{3/2})^2$  pickup. One can in Table III and IV see that this is the case for the ground state transition. But this simple picture vanishes for the other levels; for example an  $(s_{1/2} d_{3/2})$  pickup is predominant for the transition to the level at 1575 keV. Comparison of Table III and IV shows that calculation II leads systematically to larger  $(s_{1/2} d_{3/2})$  spectroscopic amplitudes than calculation I. The dominant configuration is always the same in both calculations, however.

The theoretical curves computed with the spectroscopic amplitudes of Table III and IV are displayed in Fig. 2, together with the experimental angular distributions. There is a general agreement with the data. However, there exists a marked discrepancy in the case of the 1575 keV transition; the maximum at around  $15^\circ$  is not reproduced and the experimental angular distribution falls off more rapidly than the calculated one. For this level, the spin is known and one does not have to worry about the identification of the experimental level with the calculated one. This disagreement does not seem to be related with the shell model calculations. Indeed, this level can be reached by an  $L=0+2$  transition; but pure  $L=0$  curve is forward peaked

and pure  $L=2$  curve is flat in the  $0-18^\circ$  region and so any  $L=0+2$  mixture can hardly predict a minimum at forward angles. It might be possible that the discrepancy observed is related to the distorted wave calculations, but this is difficult to check empirically. The same kind of discrepancy, although less marked, may be seen for the transition to the 3598 keV state for which a  $7/2$  spin was assumed. Shell-model calculations predict an  $L=2$  component but again the experimental differential cross-sections do not follow the predicted shape and instead show a maximum at  $14^\circ$ . The fit to the ground state is reasonably good, although the amount of  $L=0$  seems to be overpredicted at forward angles. The opposite comment applies for the 3421 keV level. For the 2717 keV level, more  $L=2$  strength is needed in order to represent the data correctly. Both sets of shell model wave functions lead in general to the same shape except for details. However this is not the case for the 2938 keV level; set I gives a better overall agreement for the 2938 keV angular distribution than set II, the reason of that being a larger  $L=0$  strength.

In Table V, we show the ratio of experimental to calculated cross-sections (which is the  $D_0^2$  coefficient, as mentioned in Section III). For both shell-model calculations the goodness of the wave functions can be judged by the constancy of  $D_0^2$ . One can see from Table V that the value of  $D_0^2$  is constant to within a factor of two for both sets. One exception is to be noted for the comparison of data for the

2938 keV level with the prediction of calculation II. In this case the fit to the shape of the data is not very good either. For the 1575 keV level, normalizing the theoretical curves on backward angles gives a better agreement to the mean  $D_0^2$  value. To sum up, the present shell model calculations give a reasonable representation of our (p,  $^3\text{He}$ ) data, although some improvement are needed to represent fully the data.

Shell-model calculations (set II) predict the analogue state of the  $^{35}\text{P}$  ground state ( $1/2^+$  T=5/2) to lie at 8620 keV. Two levels (8430 and 9155 keV) have been observed in this excitation energy range. Both angular distributions are compatible with the pure L=2 theoretical curve predicted by set II, and the  $D_0^2$  values (see Table V) for these two levels do not differ strongly (30%) from each other. Thus, the distorted wave calculations with shell-model wave functions do not permit the selection of the analogue state in this situation.

#### B. Other levels

Some negative-parity levels have been observed in our experiment. Of the levels predicted by Erne<sup>8</sup> or Maripuu and Hokken,<sup>9</sup> only the first one ( $7/2^-$ ) seems to be observed. The second negative-parity level  $3/2^-$  does not seem to be significantly excited. The appearance at 3802 keV of a second  $3/2^-$  level not predicted in either of the calculations cast some doubt about the validity of an  $^{32}\text{S}$  core hypothesis. More likely other components like  $[(s_{1/2})^{-1}(d_{3/2})^3(fp)]$  and  $[(d_{5/2})^{-1}(d_{3/2})^3(fp)]$

have to be included in the calculations. Looking at Table II, one can see that the cross sections of the negative parity levels are in general small. Some exceptions are to be noted for the tentative assignments for the 5550, 6654 and 8103 keV levels, which are relatively strongly excited. It might be possible that the main structure of these levels is built on holes in the  $1p$  shell or that the L assignments are incorrect.

#### V. CONCLUSION

In the present paper, we have reported some additional information on  $^{35}\text{S}$ . New levels have been observed and the distorted wave calculations have permitted angular momentum transfer determination for several transitions. We have attempted to reproduce the experimental cross-sections with distorted wave calculations based on two sets of shell model wave functions. However, few positive-parity levels have well established spin, so only the first six angular distribution to positive-parity levels have been analyzed. An anomaly has been noted for the 1575 keV transition which seems to be related to reaction mechanism problems. The overall agreement of the cross sections calculated with two sets of wave functions with the data is good but some details are wrong. Neither set of wave functions is clearly superior to the other on the basis of the present analysis. Further information on  $^{35}\text{S}$ , especially spins and parities for the low lying levels will allow a fuller understanding and utilization of the data presented in this work.

## ACKNOWLEDGEMENTS

One of the authors (A.G.) wishes to thank Centre National de la Recherche Scientifique and N.A.T.O. for support while on leave of absence from Institut de Physique Nucleaire de Lyon (FRANCE). The assistance of A. Saha with the experimental measurements is gratefully acknowledged.

## REFERENCES

1. C. F. Moss, Nucl. Phys. A131, 235(1969).
2. J. G. van der Baan and H. G. Leighton, Nucl. Phys. A170, 607(1971).
3. Th. W. van der Mark and L. K. Ter Veld, Nucl. Phys. A181, 196(1972).
4. L. K. Ter Veld and Th. W. van Der Mark, Phys. Rev. 173, 1101(1968).
5. F. W. Prosser and G. I. Harris, Phys. Rev. C4, 1611(1971).
6. K. S. Burton and L. C. McIntyre, Jr., Nucl. Phys. A154, 551(1970).
7. Kotalis, et al., Izo, Akad. Nauk. 35, 1684(1971).
8. F. C. Erne, Nucl. Phys. 84, 91(1966).
9. S. Maripuu and G. A. Hoken, Nucl. Phys. A141, 481(1970).
10. P.W.M. Glaudemans, G. Wiechers and P. J. Brussaard, Nucl. Phys. 56, 529, 548(1964).
11. B. H. Wildenthal, E. C. Halbert, J. B. McGroxy and T.T.S. Kuo, Phys. Rev. C4, 1266(1971).
12. B. Vignon, J. F. Bruandet, N. Longequeue, and I. S. Townner, Nucl. Phys. A162, 82(1971).
13. G. W. Greenlees and G. J. Pyle, Phys. Rev. 149, 836(1966).
14. P. D. Kunz, University of Colorado, unpublished.
15. B. F. Bayman and A. Kallio, Phys. Rev. 156, 1121(1967).
16. H. P. Morsch and R. Santo, Nucl. Phys. 172, 401(1972).
17. H. W. Baer, et al., Ann. of Phys. 76, 437(1973).
18. V. Gillet and N. Vinh-Mau, Nucl. Phys., 54, 321(1964).



19. P. M. Endt and C. van Der Leun, Nucl. Phys. A214, 333(1973).
20. H. Mann and B. H. Wildenthal, unpublished.
21. B. H. Wildenthal and W. Chung, unpublished.

## FIGURE CAPTIONS

- Fig. 1.--Energy spectrum for the reaction  $^{37}\text{Cl}(p, ^3\text{He})^{35}\text{S}$  at  $15^\circ$ .
- Fig. 2.--Angular distributions for the transitions to six low-lying positive parity states in  $^{35}\text{S}$  populated in the  $^{37}\text{Cl}(p, ^3\text{He})$  reaction. The curves represents DWBA calculations with the shell model wave-functions of calculation I (solid curve) and calculation II (dashed curves).
- Fig. 3.-- $^{35}\text{S}$  angular distributions for miscellaneous levels in  $^{35}\text{S}$ . The curves are DWBA fits to the data.
- Fig. 4.--Comparison of the experimental and calculated level schemes of  $^{35}\text{S}$  below 5 MeV. The calculated levels (of positive parity only) comes from Ref. 11 (Calc I) and from Ref. 21 (Calc II).

Table I.--Optical potential parameters used in the DWBA calculations.

	V (MeV)	$r_R$ (fm)	$a_R$ (fm)	W (MeV)	W' (MeV)	$r_I$ (fm)	$a_I$ (fm)	$r_C$ (fm)
proton	47.5	1.20	0.70		13.0	1.25	0.70	1.25
<sup>3</sup> He	173.9	1.15	0.72	20.6		1.50	0.82	1.40
n,p transferred nucleus	variable	1.20	0.60					

TABLE II.--<sup>35</sup>S spectroscopic information

Ref. 19 $E_x$ (keV)	$J^\pi$	(p, <sup>3</sup> He) $E_x$ (keV)	Level $n^\circ$	this work L	$\sigma_{max}$ ( $\mu$ b/sr)	$E_x$ (keV)	(d,p) Ref.
0	$3/2^+$	0	0	0+2+4	26.5	0	
1572.2 $\pm$ 0.12	$1/2^+$	1575	1	0+2	1.2	1575 $\pm$ 9	
1991.5 $\pm$ 0.7	$(\frac{5}{2}, \frac{7}{2})^-$	1992	2	3+5	1.5	1994.6 $\pm$ 1	
2347.6 $\pm$ 0.2	$3/2^-$					2336 $\pm$ 10	
2718.0 $\pm$ 0.6	$(\frac{3}{2}, \frac{7}{2})^-$	2717	3	0+2+4	53.9	2726 $\pm$ 8	(2
2939 $\pm$ 3	$(\frac{3}{2}, \frac{5}{2})^-$	2938	4	0+2+4	29.2	2939 $\pm$ 10	
3421.0 $\pm$ 1	$(\frac{3}{2}, \frac{7}{2})^-$	3421	5	0+2+4	81.5	3415 $\pm$ 12	
3563 $\pm$ 3						3555 $\pm$ 9	
3598 $\pm$ 2		3598	6	2+4	27.8	3595 $\pm$ 9	
(3675 $\pm$ 10)						3675 $\pm$ 10	
3802.2 $\pm$ 0.3	$3/2^-$	3811	7	3	2.6		
3818 $\pm$ 3							
3886 $\pm$ 2						(3866 $\pm$ 10)	
(3907 $\pm$ 10)						(3907 $\pm$ 10)	
4025.5 $\pm$ 1.5		4027	8	2	2.9	4025 $\pm$ 10	
4108 $\pm$ 2		4114	9	0+2	8.8	4105 $\pm$ 10	
4189.9 $\pm$ 0.3	$(\frac{1}{2}, \frac{3}{2})^-$	4186	10	(2,3)	5.6	4196 $\pm$ 12	
4304 $\pm$ 3		4290	11	(2)	2.8	4312 $\pm$ 12	
4482 $\pm$ 2		4489	12	2	2.7		
4575 $\pm$ 8		4577	13	0+2	10.7		
		4617	14	(2, 1)	13.2		
4837 $\pm$ 8		4843	15	2	15.9		
4903.5 $\pm$ 0.3		4963	16	(0+2)	17.3		
4963.2 $\pm$ 0.3		4990	17	0+2	19.5		

Ref 19 E <sub>x</sub> (keV)	J <sup>π</sup>	(p, <sup>3</sup> He) E <sub>x</sub> (keV)	Level n°	this work L	σ <sub>max</sub> (μb/sr)	E <sub>x</sub> (keV)	(d,p)	Ref. 2 k <sub>n</sub>
5058 <sup>±</sup> 8								
5126 <sup>±</sup> 11		5127	18	2	3.5			
5342 <sup>±</sup> 8		5345	19	3	2.2			
(5475 <sup>±</sup> 10)								
(5542 <sup>±</sup> 8)		5550	20	(3)	6.2			
		5771	21	2	10.1			
5980 <sup>±</sup> 10		(5915)	22	(2,3)	3.4			
6078.3 <sup>±</sup> 0.5		129	23	0+2	7.8			
6292 <sup>±</sup> 8		347	24	(2)	4.8			
6334 <sup>±</sup> 8								
6446 <sup>±</sup> 8								
6496 <sup>±</sup> 8								
6543 <sup>±</sup> 8								
6584 <sup>±</sup> 8								
6634 <sup>±</sup> 8		6654	25	(3)	7.7			
6677 <sup>±</sup> 8		6696	26	2	6.7			
6892 <sup>±</sup> 10								
7022 <sup>±</sup> 10		(7151)	27	(4)	3.3			
		(7375)	28					
		(7712)	29	4	4.6			
		7770	30		5.5			
		8103	31	(1+3)	10.6			
		8160	32	(1)	8.4			
		8430	33	2	5.7			
		9155	34	2	10.0			

TABLE III.--Spectroscopic amplitudes for <sup>37</sup>Cl+A=35 computed with wave functions obtained in calculation I.

J <sup>π</sup> B	T <sub>B</sub>	E <sub>x</sub> (MeV)	J	T	(D5,D5)	(S1,S1)	(D3,D3)	(D5,S1)	(D5,D3)	(S1)
1/2 <sup>+</sup>	3/2	1.88	1	0	0.0731	0.0677	-0.008	-0.1913	-0.008	-0.1913
			2	1	0.1208		-0.0371	0.1144	-0.2273	0.
3/2 <sup>+</sup>	3/2	0.0	0	1	0.2136	0.0825	0.5129			
			1	0	0.1075	0.0250	-0.7085	-0.0725	0.	0.
			2	1	0.0900		1.2184	0.1395	0.6633	0.
			3	0	0.0164		-1.0973	0.0252	0.1072	
3/2 <sup>+</sup>	3/2	2.79	0	1	-0.0671	-0.0984	-0.0266			
			1	0	-0.1301	-0.1816	0.1054	0.3483	0.	0.
			2	1	-0.0032		-0.0782	0.1632	-0.0455	-0.
			3	0	0.0622		0.0069	0.0436	-0.0534	
5/2 <sup>+</sup>	3/2	1.94	1	0	0.1601	0.2184	0.0163	-0.6979	-0.	-0.
			2	1	-0.0942		-0.0213	-0.0649	0.3435	-0.
			3	0	0.0319		0.0082	0.0051	-0.5144	
			4	1	0.1257				0.8806	
5/2 <sup>+</sup>	3/2	2.87	1	0	-0.1921	-0.2818	-0.0719	0.4444	-0.	-0.
			2	1	-0.1223		0.0491	-0.1769	-0.5448	-0.
			3	0	-0.0150		-0.0382	-0.0194	0.2054	
			4	1	-0.0077				-0.0963	
7/2 <sup>+</sup>	3/2	3.09	2	1	-0.1170		0.0685	-0.1838	-0.5739	-0.
			3	0	0.0058		-0.0102	0.1098	-0.0398	
			4	1	-0.0233				0.2275	
			5	0	-0.0165					

TABLE IV.--Spectroscopic amplitudes for  $^{37}\text{Cl}+A=35$  computed with wave functions obtained in calculation II.

$J_B$	$T_B$	$E_x$ (MeV)	$J$	$T$	(D5,D5)	(S1,S1)	(D3,D3)	(D5,S1)	(D5,D3)	(S1,D3)	
1/2 <sup>+</sup>	3/2	1.44	1	0	0.0008	0.0515	-0.0063	-0.1126	-0.5913		
			2	1	0.1242	-0.0062	0.1491	-0.1051	0.6036		
3/2 <sup>+</sup>	3/2	0.0	0	1	0.2169	0.1284	0.5488	-0.0422	0.1261		
			1	0	0.0865	0.0369	-0.7405	1.2537	0.1557	0.0096	-0.0279
			2	1	0.0721			1.2537	0.1557	0.0096	-0.0279
3/2 <sup>+</sup>	3/2	3.07	3	0	0.0264		-1.1386	0.0281	0.0904		
			0	1	-0.0074	0.0860	-0.0991				
			1	0	-0.0434	-0.1618	0.1258	0.1248	0.4864		
5/2 <sup>+</sup>	3/2	2.40	2	1	0.0758		-0.1544	0.0123	-0.0383	-0.3106	
			3	0	-0.0445		-0.0072	-0.0125	0.5195		
			4	1	-0.0959			-0.0214			
			1	0	-0.1201	-0.3039	0.0078	0.6044	0.3871		
5/2 <sup>+</sup>	3/2	3.27	2	1	-0.1010		0.0304	-0.1428	-0.4011	0.4149	
			3	0	-0.0378		0.0283	-0.0846	0.5195		
			4	1	-0.0195			-0.5651			
			1	0	-0.1255	-0.4369	-0.0356	0.3488	-0.0290		
7/2 <sup>+</sup>	3/2	3.31	2	1	-0.1543		0.0496	-0.2646	-0.2357	-1.0868	
			3	0	-0.0288		-0.0632	-0.0837	0.0455		
			4	1	-0.0035			-0.0300			
			5	0	-0.0236						
			1	0	-0.1134		0.0116	-0.1919	-0.0346	-1.2775	

TABLE V.--Ratio of experimental and theoretical cross-sections for the two different sets of shell-model wave functions.

$E_x$ (keV)	$J^\pi$	Set I	$\sigma_{\text{exp}}/\sigma_{\text{DW}}$	Set II
0	3/2 <sup>+</sup>	20		18
1575	1/2 <sup>+</sup>	60 <sup>a</sup> , 35 <sup>b</sup>		32 <sup>a</sup> , 17 <sup>b</sup>
2717	(5/2 <sup>+</sup> )	28		27
2938	(3/2 <sup>+</sup> )	36		55
3421	(5/2 <sup>+</sup> )	34		26
3598	(7/2 <sup>+</sup> )	27		20
8430	(1/2 <sup>+</sup> T=5/2)			16
9155	(1/2 <sup>+</sup> T=5/2)			21

a) Value obtained for a fit to forward angles.

b) Value obtained for a fit in the 30-50° angular range.

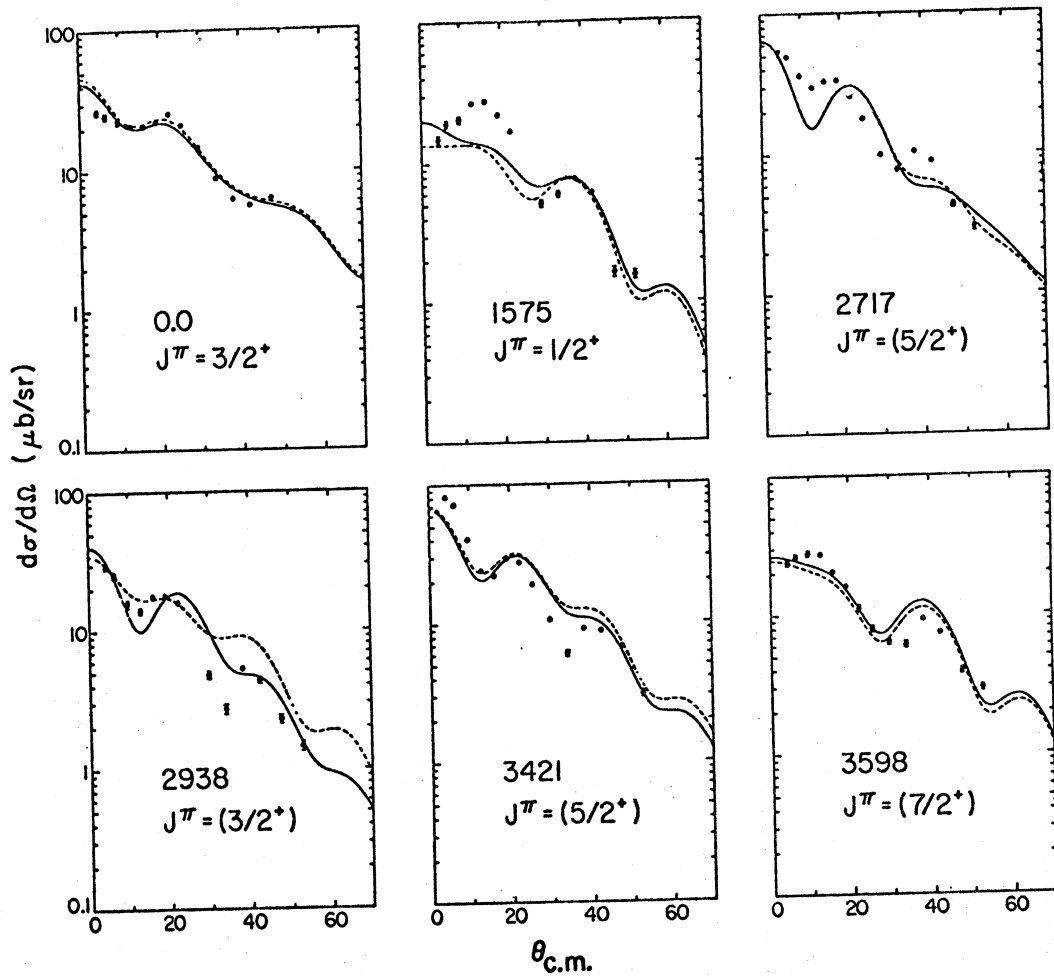


Fig. 2

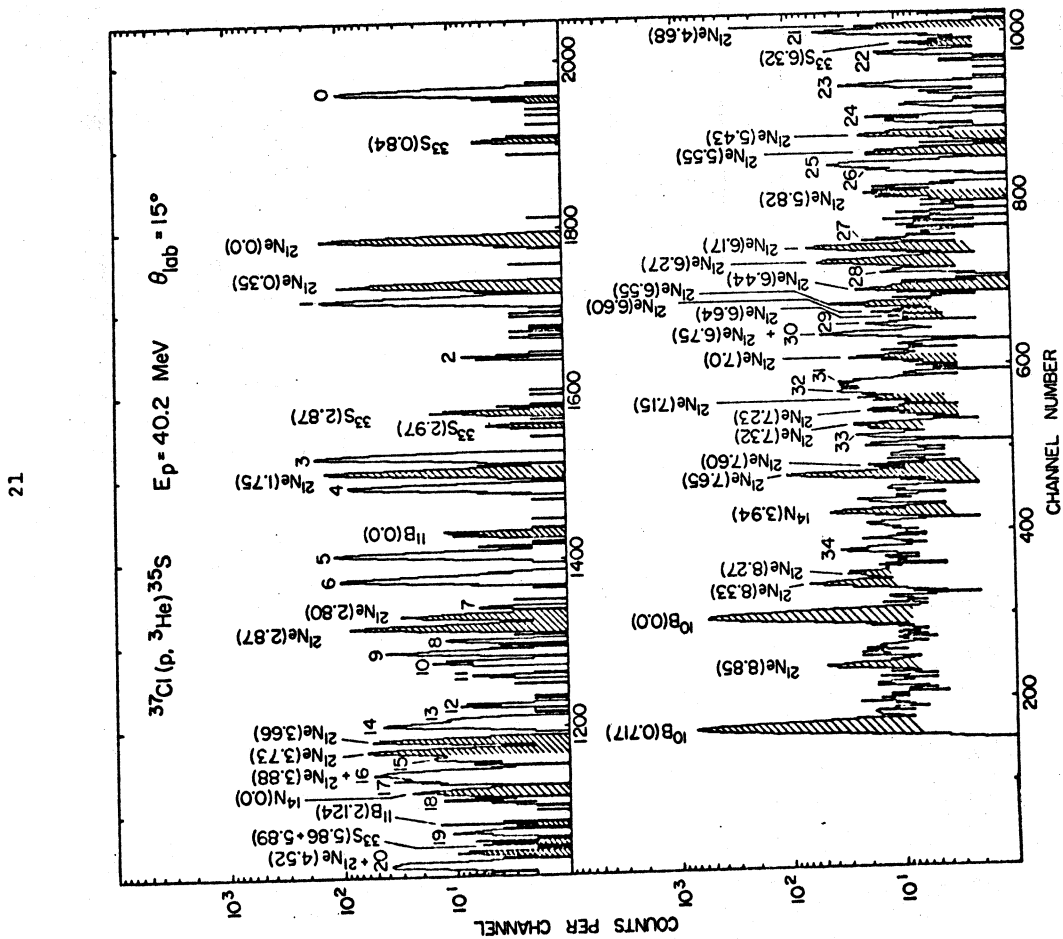


Fig. 1

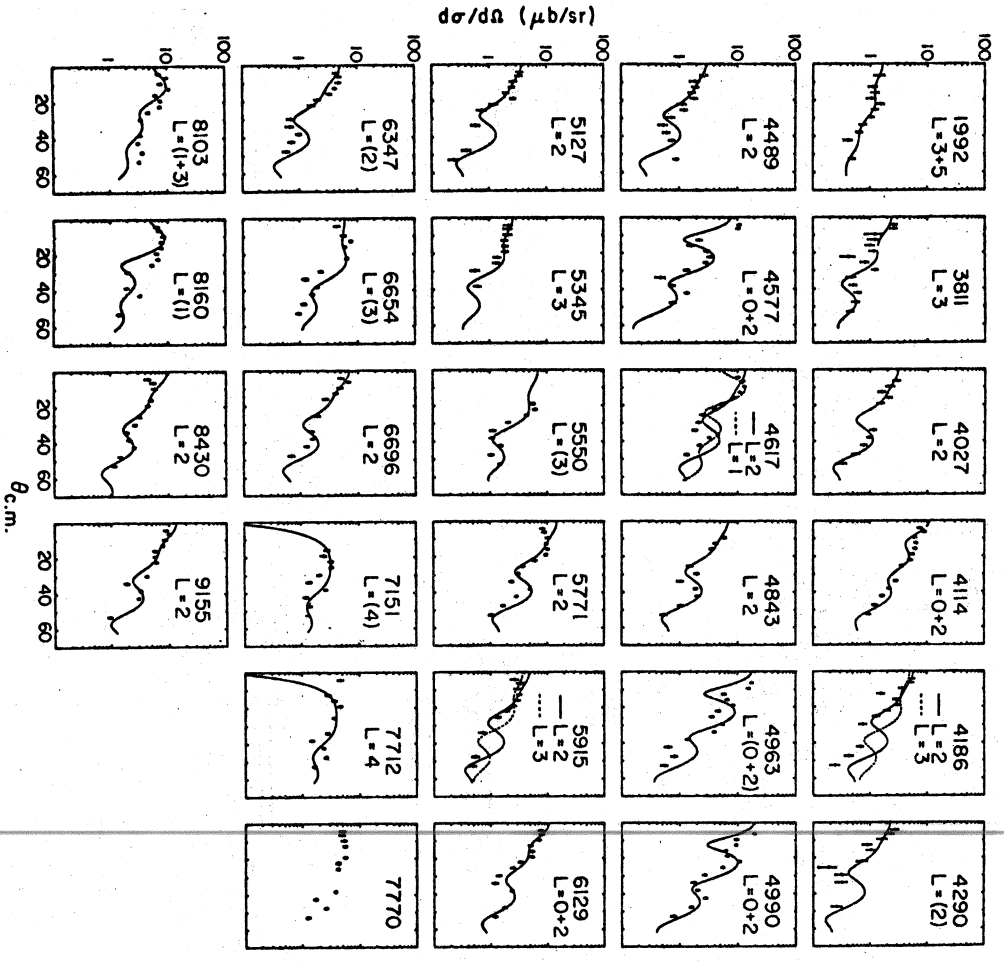


Fig. 3

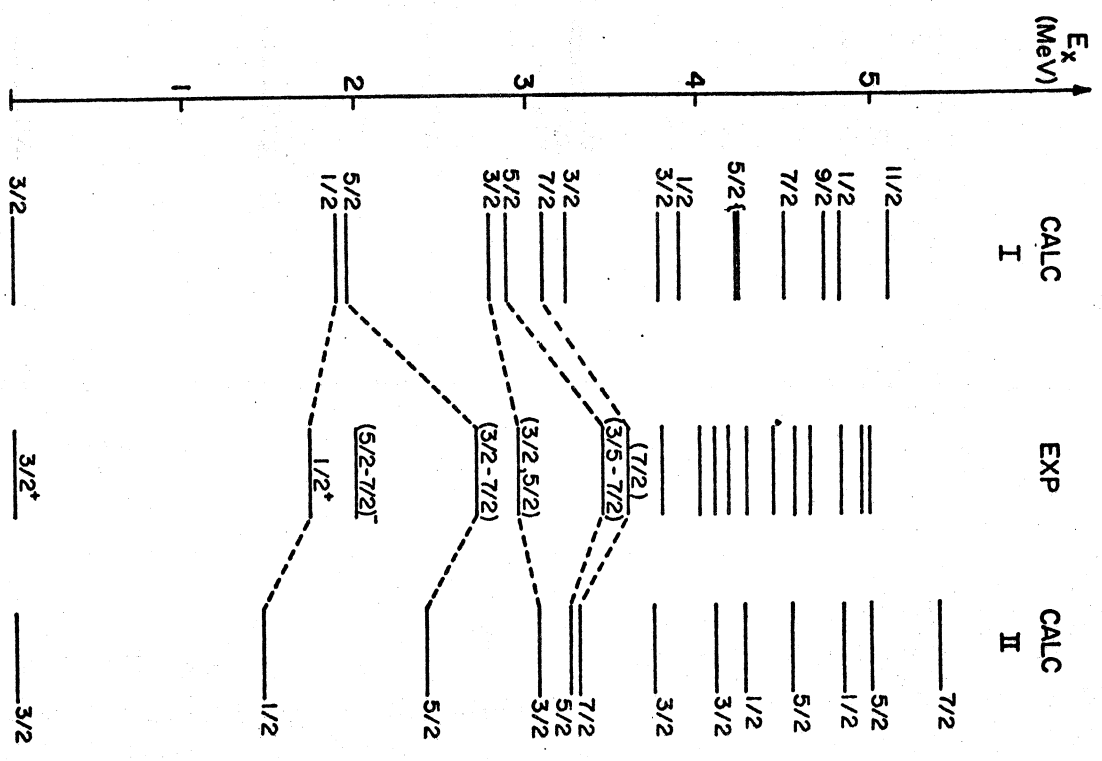


Fig. 4